

UNIVERSITÀ COMMERCIALE “LUIGI BOCCONI”

MAFINRISK

Master of Quantitative Finance and Risk Management

XVIII Cycle

**Group 5 Assignment**

**Numerical Methods**

10052 Numerical Methods

Professors: Francesco Rotondi, Gianluca Fusai

Enrico Bacchetti  
Marco Lingua  
Wei-Shiuan Su

Academic Year: 2021 - 2022

## 1 Executive Summary

The aim of this report consists of an application of numerical techniques to real-world financial data. The task can be split into two parts: the first one is devoted to the calibration of the so-called SABR model to a series of option prices on the Tesla stock<sup>1</sup>; this is done with the goal of estimating and interpolating the volatility smile implied by market quotes. The second part, based on the result of the previous one, focuses on the pricing of an Arithmetic Asian Option built on the dynamics of the SABR model. This has been done by means of MC simulation techniques applied to the discretized processes (Euler scheme).

For the convenience of the reader, the structure of the report is reported as follows. The first Section (2) contains a theoretical introduction to the SABR model. Section 3 presents the option dataset used in the analysis and details the steps followed for building it; in addition, all the assumptions concerning the data are made explicit. Next, Section 4 presents the calibration procedure of the model together with the related results. Section 5 carefully addressed the issue of how the different parameters of the SABR (namely  $\alpha, \beta, \rho, \nu$ ) and the initial forward price  $F(0)$  affected the shape, the curvature and the steepness of the implied volatility smile. Finally, Section 6 contains the second part explained above, consisting of the pricing of the exotic derivatives instrument.

## 2 Introduction

In this Section we briefly introduce the aim of our work, which consists in the calibration of a SABR<sup>2</sup> model to a bunch of options on TSLA and in the subsequent pricing of an exotic derivatives product at our choice.

The SABR is a widespread model in the industry, largely used for identifying skews and smiles characteristics in the implied volatility surface of options instruments. The dynamics of the SABR model are given by the following two stochastic differential equations:

$$dF_t = \alpha_t F_t^\beta dW_t^1 \quad F(0) = f \quad (1)$$

$$d\alpha_t = \nu \alpha_t dW_t^2 \quad \alpha(0) = \alpha \quad (2)$$

where the underlying forward price is assumed to follow the CEV dynamics and  $\alpha, \beta$  ( $0 \leq \beta \leq 1$ ),  $\rho$  and  $\nu$  are the four parameters of the model. The two risk factors (i.e. the two Brownian Motion processes) are correlated according to  $E[dW_1, dW_2] = \rho dt$ , with  $-1 \leq \rho \leq 1$ .

The appeal of the model lies in the so-called *Hagan's formula* (function of the strike  $K$  and the maturity  $T$ )

that allows computing implied volatilities in a closed-form way. For the sake of completeness, we include it in Equation 3, together with all its building components.

$$\sigma_H(T, K) \approx a(K)b(T, K) \left( \frac{c(K)}{g(c(K))} \right) \quad (3)$$

where:

$$\begin{aligned} a(K) &= \alpha \left[ (FK)^{(1-\beta)/2} \left( 1 + \frac{(1-\beta)^2}{24} \log^2 \frac{F}{K} + \frac{(1-\beta)^4}{1920} \log^4 \frac{F}{K} \right) \right]^{-1} \\ b(K) &= \left[ 1 + \left( \frac{(1-\beta)^2}{24} \frac{\alpha^2}{(FK)^{1-\beta}} + \frac{\rho\beta\nu\alpha}{4(FK)^{(1-\beta)/2}} + \frac{2-3\rho^2}{24} \nu^2 \right) T \right] \\ c(K) &= \frac{\nu}{\alpha} (FK)^{(1-\beta)/2} \log \frac{F}{K} \\ g(x) &= \log \left( \frac{\sqrt{1-2\rho x + x^2} + x - \rho}{1-\rho} \right) \end{aligned}$$

## 3 Dataset and Assumptions

In the present Section we carefully explain the assumptions we have made in order to carry out our project and the steps followed in building the initial dataset. First, as for the options' *underlying* we opted for the *Tesla* stock (Ticker: TSLA). The choice was mainly driven by the fact that we wanted to work with an equity instrument that proved to be rather volatile over the recent periods (see Figure 1), to exploit at best the smiles and skew features of its implied volatility curve; moreover, TSLA is a very liquid and traded stock and the same holds for its related derivatives instruments.



Figure 1: Tesla Implied Volatility (Source: [1])

Second, the dataset is based on end-of-day options data (both calls and puts as of 29th March 2022) collected from Yahoo Finance and downloaded with the .py code submitted alongside with the report.

<sup>1</sup>In the financial literature, the SABR model is usually employed for calibrating parameters of non-linear models related to interest rates, exchange rates or equity.

<sup>2</sup>The acronym SABR stands for Stochastic Alpha Beta Rho

The script allows the user to get filtered data, as it includes some preliminary selection criteria concerning the *open interest* and the *implied volatilities*. More specifically, we considered a threshold value for the open interest (fixed at 400<sup>3</sup>, based on the empirical analysis of the variable for TSLA) as a lower bound for the options picking strategy. This allows to exclude from the dataset the less liquid instruments which could entail biases in the estimation procedure and produce anomalous discrepancies between model implied volatilities and market quotes (see [3]).

Furthermore, we observed that raw data may present incoherences for what concerns the implied volatilities: in particular, the data provider sometimes quotes values of 0.0001% for certain options. These irregularities have been kept into consideration by removing the corresponding observations from the dataset.

After this initial data-handling process, the data are imported into the Excel file where a twofold assessment, related to *moneyness* and *maturity*, has been applied<sup>4</sup>. As for the moneyness, we decided to go for OTM options only, since they are known to be much more liquid than the ITM ones.

As for the maturity, instead, we have focused on options whose expiration date is the 17th of March, 2023 ( $T = 0.9644$ ). First of all, this choice was again driven by liquidity considerations, as we have retained one of the maturities with the highest *average* open interest. Secondly, the main findings in the literature do support the use and the reliability of the SABR model primarily for short-term time horizons (from 1 to 12 months) (see [9] and [7]); as such, we opted for the one-year maturity because it falls within this range.

At the end of all the explained process, our final dataset consists of 1669 (72 of which belong to the one-year maturity and 49 of them are OTM) observations, each of them displaying values for eight different variables: ID, strike, open interest, implied volatility, moneyness, days to expiration, type (call/put) and market price (average between the bid and ask quote).

Other noteworthy operational assumptions and remarks relate to the *risk-free rate* and the *initial forward price* ( $F_0$ ). More specifically, the former has been computed

as a linear interpolation of a selected term-structure of interest rates (LIBOR rates as 29<sup>th</sup> March 2022 downloaded from [2]); the latter, instead, has been computed by applying the standard forward price formula ( $F = S(0)e^{rT}$ ) with  $S(0)$  taken again as the closing price on the 29<sup>th</sup> March, 2022.

## 4 Calibrating SABR

In order to obtain an estimate of the different SABR parameters, we proceed by using the *Non Linear Least Squares* procedure (NLLS), i.e. by minimizing the squared errors between the model implied volatilities  $\sigma_H(T, K, \theta)$  (where  $\theta = \{\alpha, \beta, \rho, \nu\} \in \mathbb{R}^4$  is the set of parameters) and the market empirical counterparts  $\sigma_{MKT}$ . The optimization procedure consists in the solution of the following minimization problem:

$$\hat{\theta} = \underset{i=1}{\operatorname{argmin}} \sum^n (\sigma_{MKT_i} - \sigma_{H_i}(T, K_i, \theta))^2 \quad (4)$$

subject to these constraints:  $\alpha, \nu > 0$ ,  $0 \leq \beta \leq 1^5$ ,  $-1 \leq \rho \leq 1$ ;  $n$  represents instead the number of options in our dataset for the selected 1y maturity.

Market volatilities may either be extracted by the price functional of an option by means of numerical algorithms (e.g Newton-Raphson method) or directly taken from data providers. As already explained, we opted for the second option as we have built the options dataset relying fully on Yahoo Finance<sup>6</sup>. The resulting estimated smile from the optimization procedure can be appreciated in Figure 2, while the estimated parameters<sup>7</sup> are reported in Table 1 below.<sup>8</sup>

<sup>3</sup>The unit of measure of open interest is the number of outstanding contracts.

<sup>4</sup>The spreadsheet is designed to be dynamic and flexible; in particular, it autonomously selects OTM options (moneyness constraints) and allows the user the selection of a particular maturity.

<sup>5</sup>An additional remark on  $\beta$  is needed: although it can take values in that interval, in market practice it is usually fixed before calibration. More specifically, this parameter accounts for the shape of the returns density: a value of 0 implies normal returns, a value of 1 suggests lognormal returns, while a value in-between 0 and 1 points to a constant elasticity of the variance process. Usually, the choice of  $\beta$  has little effect on the calibration results but may have some meaningful impact on the options' greeks [8]. In our application, we fixed it at the 0.5 level.

<sup>6</sup>See Appendix 8 for some considerations on the numerical methods for the computation of the implied volatilities.

<sup>7</sup>The excel Solver is initialized without the parameters' constraints since it reaches the optimum returning well-behaved estimates which are coherent with the restrictions detailed above.

<sup>8</sup>This graph can give a crystal-clear overview, together with the SSR reported in Table 1, on the goodness of fit of our calibration procedure.

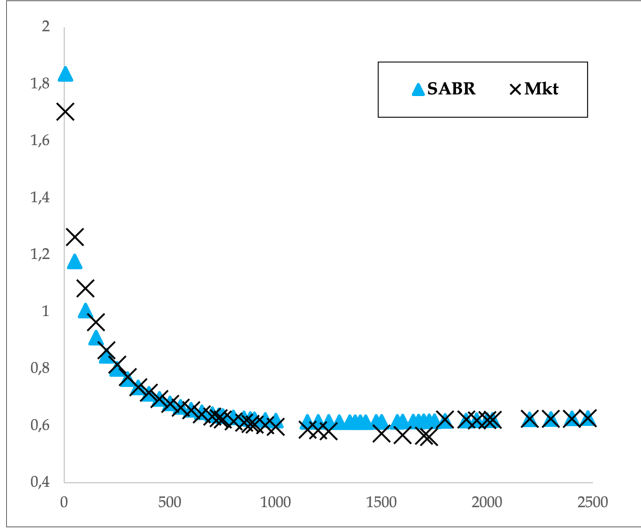


Figure 2: Empirical vs. fitted smile with SABR

Parameter	Value
$\hat{\alpha}$	19.8670
$\hat{\rho}$	0.5016
$\hat{\nu}$	0.5268
SSR	0.03890
Time (s)	10.3489

Table 1: Optimization results ( $\beta = 0.5$ )

By looking at the graph, we can clearly state that the SABR model fits well and the estimated implied volatilities closely replicate the empirical counterparts for each level of the strike  $K_i$  ( $i = 1 \dots n$ , with  $n = 49$ ). As for the estimated parameters, we can assess how  $\hat{\alpha}$  is rather large, suggesting high initial volatility of the forward price process; on the other side,  $\hat{\nu}$  (the so-called "vol-vol parameter") is rather low, suggesting a small variability in the dynamics of the  $\alpha_t$  process. Finally, the estimated correlation coefficients  $\hat{\rho}$  are positive and quite large, pointing out that the processes represented in the SDEs (Equations (1) and (2)) are quite linearly related one with the other.

As stated in [5], under given conditions, the NLLS has asymptotic normality properties, namely  $\hat{\theta} - \theta \sim \mathcal{N}(0, \frac{\sigma^2}{n} \mathbf{Q}^{-1})$ , where  $\mathbf{Q}$  is the asymptotic variance-covariance matrix and  $\sigma$  is the standard deviations of the true errors. Since these are unknown quantities, they are consistently estimated by, respectively,  $\frac{s^2}{n} (\mathbf{H}'\mathbf{H})^{-1}$  and  $s = \frac{1}{n-k} \sum_{i=1}^n (\sigma_{MKT_i} - \sigma_{H_i})^2$ , where  $\mathbf{H}$  is the Jacobian matrix and  $k = 3$  is the dimension of the parameters set (note again that  $\beta$  has been fixed to 0.5 and has not entered the estimation procedure).

In order to compute the Jacobian matrix, which in-

cludes, for the different  $K$ s, the first partial derivatives of  $\sigma_H(K)$  with respect to the three estimated parameters  $\alpha, \rho$  and  $\nu$ , we have followed a numerical method estimating them via the *centered finite differences* approach. In particular, for a generic function  $f = f(x, y)$ , the partial derivative with respect to  $x$  is approximated as:

$$\frac{\partial f(x, y)}{\partial x} \approx \frac{f(x + h, y) - f(x - h, y)}{2h} \quad (5)$$

for any small number  $h$  (in our case  $h = 0.00001$ ). The computed partial derivatives have been grouped into the  $n \times 3$  *Jacobian matrix*, whose generic  $ij$ -th element is given by:

$$\mathbf{H}_{ij} = \frac{\partial \sigma_H(K_i, \hat{\theta})}{\partial \theta_j} \quad j = 1, 2, 3 \quad i = 1, \dots, 49 \quad (6)$$

Tables 2 and 3 contain respectively an extract of the final Jacobian matrix and of the corresponding asymptotic variance-covariance matrix  $\hat{\mathbf{Q}}^{-1} = \frac{s^2}{n} (\mathbf{H}'\mathbf{H})^{-1}$ .

i	$\frac{\partial \sigma_H}{\partial \alpha}$	$\frac{\partial \sigma_H}{\partial \rho}$	$\frac{\partial \sigma_H}{\partial \nu}$
1	0.0008	0.090	1.2183
2	0.0008	0.0199	1.2169
3	0.0007	0.0299	1.2159
i	...	...	...
49	0.0008	-0.0299	1.2264

Table 2: Extract of the Jacobian matrix  $\mathbf{H}$ 

	$\hat{\alpha}$	$\hat{\rho}$	$\hat{\nu}$
$\hat{\alpha}$	2.3834E-01	1.0548E-03	-1.7929E-04
$\hat{\rho}$	1.0548E-03	1.1456E-05	-4.9270E-08
$\hat{\nu}$	-1.7929E-04	-4.9270E-08	3.8732E-07

Table 3: Consistent estimate of  $\mathbf{Q}$ 

As can be seen in Table above, estimates come with fairly low variances and covariances, and this is a suggestion of the goodness of fit of the calibration procedure.

## 5 Smile and parameters

In the current Section, we provide a detailed summary of how the implied volatility smiles arising from our calibrated SABR model react when changing (in either direction) one of the three estimated parameters  $\hat{\alpha}, \hat{\rho}, \hat{\nu}$  and the current forward price  $F(0)$  of the options' underlying.

Figures 3, 4, 5, 6 and 7 report the volatility smile when

shocking the above-mentioned parameters as reported in the legends accompanying the graphs. On the x-axis, the reader can find the range of strikes, while on the y-axis the specific parameter values' scale is reported.<sup>9</sup>

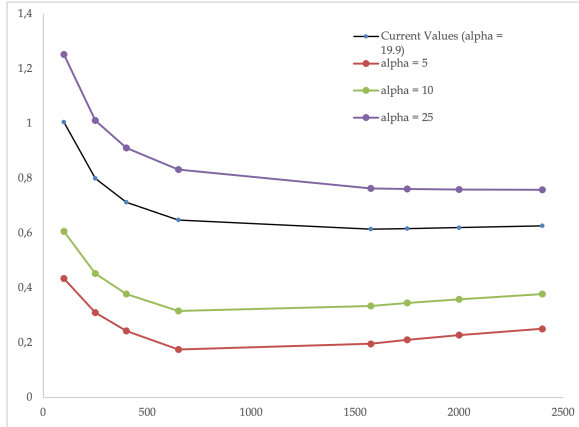


Figure 3: SABR implied volatility and  $\alpha$

In Figure 3 the dark blue line reflects the  $\alpha$  value estimated with the SABR (i.e. 19.8670). As we can see from the other curves, as the value of the parameter is changed in one direction (upward or downward), the IV smile tends to co-move in the same way<sup>10</sup> (upward or downward). This is a typical pattern concerning the  $\alpha$  parameter.

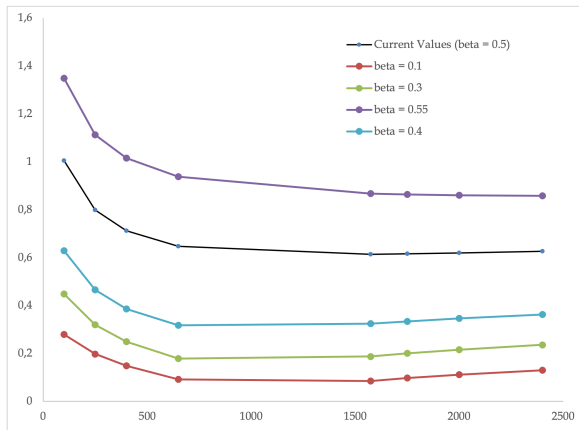


Figure 4: SABR implied volatility and  $\beta$

In Figure 4 some selected IV smiles for different values of  $\beta$  are displayed. It is immediate to notice how the smile is affected in almost the same way as when shocking  $\alpha$ . As its magnitude is increased from our baseline scenario towards 1 (upper bound), the IV smile shifts upwards;

vice versa for decreasing values towards 0 (lower bound) the position of the smile is displaced downwards.

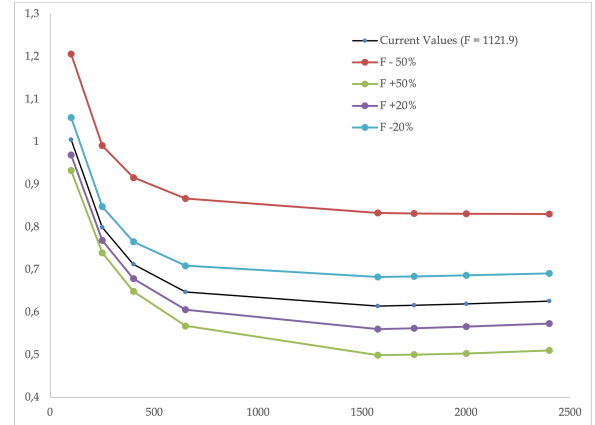


Figure 5: SABR implied volatility and  $F(0)$

Figure 5 shows the pattern of the IV smile when changing the forward price of the options' underlying  $F(0)$ . As we can see also here, the behaviour of the smile resembles in some sense the one detected for  $\alpha$  with the only difference that the shift is restrained for small strikes and amplified for higher values of  $K$ . This observed fact in our dataset slightly detaches from the empirical evidence, since one would expect (as reported in [4]) the smile to move to the right when increasing the forward rate (and vice versa).

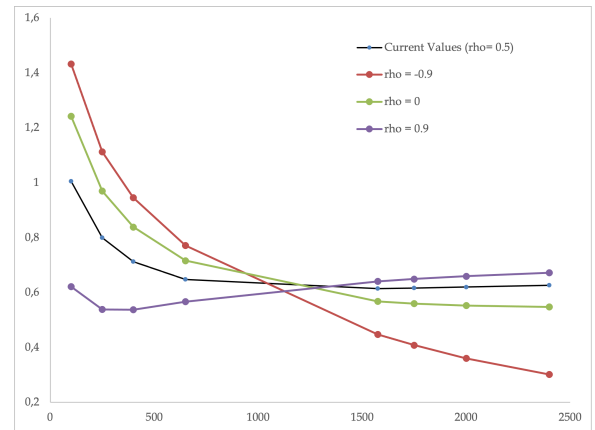


Figure 6: SABR implied volatility and  $\rho$

In Figure 6 we report the IV smile's changes given a change in the  $\rho$  parameter. As expected, the smile becomes more negatively sloped the more negative the correlation parameter<sup>11</sup>, while for positive values of  $\rho$  the

<sup>9</sup>We provide these graphs since we believe are a powerful tool to understand how different variables and parameters affect the behaviour of the smile.

<sup>10</sup>The  $\alpha$  parameter is also known as the *shift* parameter.

<sup>11</sup> $\rho$  is also known as *leverage* parameter

curve shows a slightly positive slope.

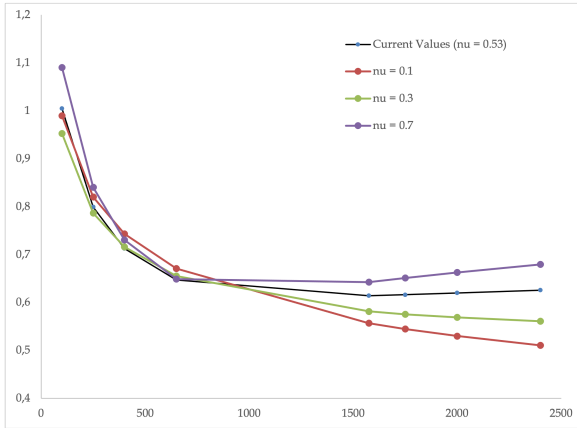


Figure 7: SABR implied volatility and  $\nu$

Finally, Figure 7 plots the IV smile for some selected values of  $\nu$ , the vol-vol parameter. Again, also in this last case, the IV smile behaves in the same way as the majority of empirical evidence suggests. Indeed, its (convex) curvature becomes more pronounced by increasing  $\nu$ .

To sum up, the interaction between these four parameters allows obtaining different volatility shapes in terms of smile level, steepness and curvature.

## 6 MC Option Pricing with SABR

Once the calibration procedure has been concluded, we addressed the exotic derivative pricing task. More specifically, we relied on Monte Carlo (MC) techniques to jointly simulate the forward price and the stochastic volatility processes, then used them to price a *path-dependent* Asian call option, whose payoff is reported in Equation (7) below:

$$X(T) = \text{MAX} \left( F(T) - \frac{1}{n_t} \sum_{t=1}^T F(t); 0 \right) \quad (7)$$

where  $n_t$  represents the number of monitoring days (241 for our selected maturity). The peculiarity of this exotic option is that it does not consider a constant pre-determined value as strike price (like in plain vanilla options), but the arithmetic mean of all the underlying future prices recorded in all the  $n_t$  monitoring days, i.e. from  $t = 0$  to  $t = T$ .

Our starting point for the simulations is the system of

SDEs described in (1) and (2), whose solution can be approximated with a good degree of precision by an Euler scheme discretization.

$$F(t + \Delta t) = F(t) + \alpha(t)F(t)^\beta (\sqrt{1 - \rho^2 \Delta t} N_1 + \rho \sqrt{\Delta t} N_2) \quad (8)$$

$$\alpha(t + \Delta t) = \alpha(t) + \nu \alpha(t) \sqrt{\Delta t} N_1 \quad (9)$$

where  $N_1$  and  $N_2$  are two independent random standard normal variables and  $\Delta(t)$  is the monitoring time-interval, computed as the ratio between the option maturity  $T$  and the number of trading days (for the convention, assumed to be equal to 250 days).

The simulation process is reported in the Excel sheets `OptionPricing`, `a(t)` and `RAND.N` where, respectively, the future price, the volatility and a matrix of random standard Normal RVs. (needed to account for the joint risk factor arising from the Cholesky decomposition in (8)) are generated. The option price at  $t = 0$  is computed as the discounted expected value of the simulated payoffs, namely:

$$\tilde{C} = E[X(T)e^{-rT}] = \frac{1}{NSim} \sum_{i=1}^{NSim} (X(T)e^{-rT}) \quad (10)$$

where  $NSim$  is the number of Monte Carlo simulations and  $r$  is the risk-free rate referred to as the maturity  $T$ . The worksheets are based on VBA macros, which have been implemented to allow the computation of a variety of numbers of simulations. Together with the MC price, we provide also the sample standard deviation  $\hat{\sigma}$  and the Monte Carlo radius (11) as measures of accuracy of the point estimate.

$$MC \text{ Radius} = z_{\frac{\delta}{2}} \frac{\hat{\sigma}}{NS} \quad (11)$$

where  $z_{\frac{\delta}{2}}$  is the  $\frac{\delta}{2}$ -quantile of a standard normal density (in our case the significance level  $\delta = 0.05$ ). By means of the Monte Carlo radius we computed the confidence interval of the point estimate, whose upper and lower bounds are given by  $\tilde{C} \pm z_{\frac{\delta}{2}} \frac{\hat{\sigma}}{NSim}$ : increasing the number of simulations, the simulated price should converge to the unknown theoretical price and the estimator quality improves. Concerning this aspect, the VBA file provides a measure of CPU runtime after the simulation is ended; in Table 4 we provide a brief overview of how increasing the number of scenarios improves the accuracy of the estimator but requires more waiting time.<sup>12</sup>

<sup>12</sup>Table 4 can help the reader on how the trade-off between the accuracy of estimates and runtime and/or computational power behaves in Monte Carlo simulations.

NSim	$\tilde{C}$	$\hat{\sigma}$	MC Radius	Time (s)
100	165.7904	435.9993	36.4155	3.5678
500	152.6527	315.4994	11.7883	5.5195
1000	153.0856	404.0909	10.6728	7.7109
5000	158.8063	381.1482	4.5020	22.6093
10000	157.0053	392.1076	3.2749	80.8767

Table 4: Pricing accuracy in a Monte Carlo framework (CPU: Intel i7 2.2 GHz)

## 7 Conclusions

In this report, we addressed the problem of the calibration of a SABR model to a series of one-year-maturity options on the Tesla stock. The criteria followed for the selection of the data (puts and calls) are carefully addressed in Section 3. By applying Hagan's formula (see Equation 3) and so estimating its three relevant parameters ( $\alpha$ ,  $\rho$  and  $\nu$ ), we were able to interpolate the implied volatility smile which is represented in Figure 2. It is immediate to notice that the fit is satisfactory for all the different levels of the strike  $K$  and this can be also proven by looking at the close-to-zero values of the components of the  $3 \times 3$  estimated asymptotic variance-covariance matrix (Table 3).

The second part of the work is carried out in Section 6 and consists of the pricing of an (invented) exotic derivatives (an Asian arithmetic payoff) with payoff as in 7. To do so, we made use of standard MC simulation techniques applied to the Euler scheme discretization of the two SDEs reported in Equations (8) and (9). The computational tasks have been developed by means of VBA and Excel; some estimated option prices with some selected numbers of simulations are reported in Table 4. A measure of accuracy and the requested computational power are also included. The last two rows of the table (5000 and 10000 simulations, which guarantee more precision) suggest a theoretical price of the instrument of around 157-158\$. Although cannot be compared with the theoretical price of the Asian option instrument given the lack of a closed-form solution, this result seems to be at least plausible and quite reliable. This statement can be justified given that many of the options included in the working dataset display "similar price"<sup>13</sup>.

<sup>13</sup>We acknowledge that this comparison must be taken with a grain of salt as no technical proof can be provided, as the moneyiness features are not available; furthermore, also the strikes represent an element that can be hardly used for the comparison

## 8 Appendix

### 8.1 Appendix A

As already stated in the main report, implied volatilities can be extracted from market quotes through different numerical techniques, such as the *Bisection* or the *Newton-Raphson* methods, the latter known to be faster than the former, even if it is not always convergent. In the table above is reported a brief example of how the two methods perform if compared to observed implied volatilities, for a selected range of strike options (see .py code).

Strike	Mkt.	Type	NR	Bisection
1150	0.632030	C	0.622906	0.622906
1500	0.624053	C	0.619998	0.620007
1750	0.621044	C	0.617256	0.617266
2000	0.620384	C	0.616838	0.616851
2400	0.624858	C	0.621642	0.621667
50	1.262698	P	NC	1.256138
100	1.083256	P	NC	1.075904
150	0.963989	P	NC	0.955976
200	0.865052	P	0.811783	0.856481
500	0.676486	P	0.663703	0.663702
750	0.622096	P	0.604528	0.604528
1000	0.596794	P	0.572761	0.572766

Table 5: Comparison between different implied volatilities (Market, Newton-Raphson and Bisection methods)

Please note that, for the above Table, we reported six decimals digits instead of four to provide the reader with a better insight into the relative difference between the volatilities for a single strike. As we can see in Table 5, both algorithms often provide consistent estimates, but the NR method does not converge for some put options with very low strike prices and observed volatility near one (please note that we are still considering the options with our selected expiration date).

### 8.2 Appendix B

In the following plots, other different meaningful graphical results obtained in the spreadsheet are reported: 15 paths of the simulated  $F(t)$  dynamic, together with their corresponding stochastic volatilities  $\alpha_t$  and the payoff histogram (zero values are not included to give the reader a better focus on the distribution of strictly positive payoffs). All the three graphs are referred to as the same simulated values, with  $NSim = 10000$ .

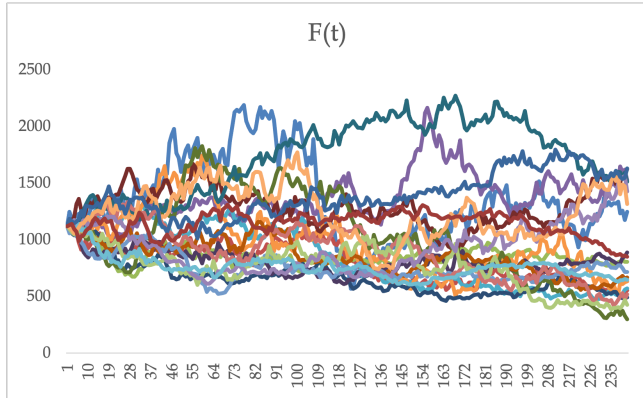


Figure 8:  $F(t)$  simulated paths (10000 simulations)

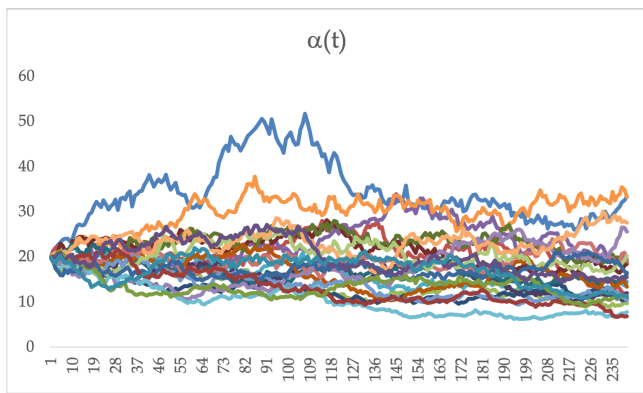


Figure 9:  $\alpha(t)$  simulated paths (10000 simulations)

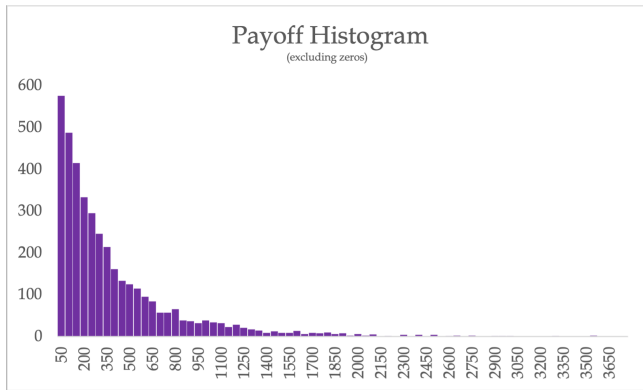


Figure 10: Distribution of simulated payoffs (10000 simulations)

## References

- [1] Tesla IV Graph (alphaquery)
- [2] Global Rates website
- [3] Chang, W., Pant, V. The Valuation of Options in Illiquid Markets: A Comparison of Methods, *SSRN*, 2003.
- [4] Fusai, G. Presentation: The Volatility Surface Università Luigi Bocconi, 2021-22.
- [5] Greene, W. H. Econometric analysis. *Upper Saddle River, Prentice Hall*, 2008.
- [6] Hagan, P., Kumar, D., Lesniewski, A., Woodward, D. E. Managing Smile Risk *Wilmott 1* (84-108), 2002
- [7] Lesniewski, A. First Baruch Volatility Workshop, New York, 2015.
- [8] Nowak, P., Sibet, P., Volatility Smile (Heston, SABR), 2012.
- [9] Rømer, S.E., Poulsen, R. How Does the Volatility of Volatility Depend on Volatility? *Risks* (8,59), 2020.
- [10] Yin, L., Monte Carlo Strategies In Option Pricing For Sabr Model, *Chapel Hill*, 2015.